Truncated Parabolic-Index Fiber with Minimum Mode Dispersion

MASAHIRO GESHIRO, STUDENT MEMBER, IEEE, MASANORI MATSUHARA, AND NOBUAKI KUMAGAI, SENIOR MEMBER, IEEE

Abstract—**The use of a parabolic-index fiber as an optical transmission line has been receiving extensive attention because of its excellent mode dispersion characteristics.**

In the present paper, the modal dispersion in the optical fiber with truncated parabolic index distribution is analyzed theoretically in detail by using a variational method. Taking the influence of the cladding upon the propagating modes into consideration, it is found that there exists an optimum index distribution for which the modal dispersion is minimized. The standard deviation of the normalized group delay of propagating modes is used to estimate the modal dispersion behavior of the fiber.

I. Introduction

MODAL DISPERSION in multimode optical fibers is caused by the differences of group velocities of each propagating mode. The modal dispersion broadens the output pulsewidth which in turn restricts the optical data transmission capabilities. It has been pointed out, experimentally and theoretically, that optical fibers with parabolic-index distribution show little modal dispersion in comparison with other optical waveguides [1], [2].

The parabolic-index fiber consists of a core with parabolic-index distribution surrounded by a cladding of constant refractive index. The influence of the cladding upon the lower order modes is negligible because their energies are trapped tightly into the core. However, the higher order modes are affected significantly by the cladding because a considerable portion of their energies propagates in the cladding [3]. Therefore, we must take the influence of the cladding upon the propagating modes into account to discuss the mode dispersion characteristics of the multimode truncated parabolic-index fiber. To the authors' knowledge, however, the detailed analysis of the mode dispersion characteristics including the effect of the cladding has not yet been reported.

In this paper, the mode dispersion characteristics of the truncated parabolic-index fiber are analyzed theoretically in detail by using a variational method [4], [5], and the optimum index distribution to achieve the minimum modal dispersion is found. To estimate the modal dispersion behavior of the fiber, the standard deviation of normalized group delay of the propagating modes is used. This standard deviation gives the output pulsewidth broadening due to the modal dispersion provided that the mode conversion effects are small.

Manuscript received December 21, 1976; revised April 25, 1977.

The authors are with the Department of Communication Engineering, Faculty of Engineering, Osaka University, Suita-shi, Yamada-kami, Osaka 565, Japan.

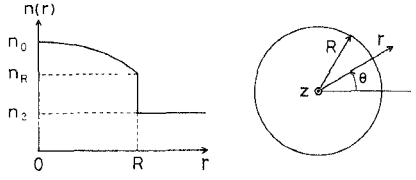

Fig. 1. Refractive-index distribution of truncated parabolic-index fiber and circular-cylindrical coordinates used in the analysis.

II. Refractive-Index Distribution and Propagating Modes

The fiber under consideration is assumed to be uniform in both the circumferential direction θ and the propagation direction z. As shown in Fig. 1, the refractive-index distribution in the radial direction r is assumed to be

$$n(r) = \begin{cases} n_1(r) = n_0[1 - ar^2]^{1/2}, & r \le R \\ n_2, & r > R \end{cases} \tag{1}$$

where R is the radius of the core, and n_0 is the refractive index at the axis ($r = 0$) of the fiber. The parameter a determines the rate of change of the refractive-index variation, and is expressed as

$$a = [1 - (n_R/n_0)^2]/R^2 \tag{2}$$

where n_R is the refractive index of the core at the boundary between core and cladding ($r = R$). As the electromagnetic fields of the waves are almost TEM, the wave equation can be expressed approximately by the following scalar wave equation [6];

$$\nabla^2\Phi + k^2n^2(r)\Phi = 0 \tag{3}$$

where Φ is the transverse electric (or magnetic) field, and k is the wavenumber in free space.

Assuming that the direction of propagation is along the z axis and β is the propagation constant, the field Φ can be expressed as

$$\Phi(r,\theta,z) = \phi(r,\theta) \cdot \exp[-j\beta z] \tag{4}$$

in which the harmonic time dependence $\exp[j\omega t]$ is omitted for brevity. Substituting (4) into (3), we get

$$\nabla^2\phi + [k^2n^2(r) - \beta^2]\phi = 0. \tag{5}$$

0018-9480/78/0200-0115$00.75

The variational expression for the propagation constant can be derived from (5) in the form [7]

$$\beta^2 = \frac{\int_S [k^2 n^2(r)\phi^2 - (\nabla\phi)^2]\, dS}{\int_S \phi^2\, dS}. \tag{6}$$

The surface integral in (6) must be carried out over the whole transverse surface and the trial function ϕ in the same equation must be continuous across the entire surface of integration.

Since most of the power of the modes is concentrated in the fiber core with parabolic-index profile, let us represent the trial function ϕ in (6) in terms of the Gauss–Laguerre function as follows:

$$\phi_{lm}(r, \theta; b) = \frac{1}{\sqrt{\varepsilon_l \pi}} \cdot \frac{\sqrt{2m!}}{\sqrt{(l+m)!}} \cdot \frac{1}{\zeta} \cdot \begin{pmatrix} \cos(l\theta) \\ \sin(l\theta) \end{pmatrix} \cdot L_m^l\left(\frac{r^2}{\zeta^2}\right) \cdot \left(\frac{r}{\zeta}\right)^l \cdot \exp\left[-\frac{r^2}{2\zeta^2}\right] \tag{7}$$

where ζ and ε_l are expressed as

$$\zeta = 1/\sqrt{kn_0\sqrt{b}} \tag{8}$$

and

$$\varepsilon_l = \begin{cases} 2, & l = 0 \\ 1, & l \neq 0 \end{cases} \tag{9}$$

respectively. $L_m^l(x)$ in (7) is a Laguerre polynomial defined by

$$L_m^l(x) = \frac{x^{-l} \cdot \exp[x]}{m!} \cdot \frac{d^m}{dx^m}(x^{m+l} \cdot \exp[-x]). \tag{10}$$

In (7) and (10), l and m are zero or positive integers which are used to label the propagating modes, and the parameter b is determined by the stationary condition of the variational expression.

Substituting (7) into (6), we get the variational expression for the propagation constant of the (l,m) mode. The result is

$$\beta_{lm}^2(b) = \hat{\beta}_{lm}^2(b) + k^2 n_0^2 \cdot \int_0^\infty f(r; b)\psi_{lm}^2(r; b) r\, dr \tag{11}$$

where

$$\hat{\beta}_{lm}^2(b) = k^2 n_0^2 - 2(2m + l + 1)/\zeta^2 \tag{12}$$

$$f(r; b) = \begin{cases} (b-a)r^2, & r \leq R \\ (n_2/n_0)^2 - (1 - br^2), & r > R \end{cases} \tag{13}$$

$$\psi_{lm}(r; b) = \frac{\sqrt{2m!}}{\sqrt{(l+m)!}} \cdot \frac{1}{\zeta} \cdot L_m^l\left(\frac{r^2}{\zeta^2}\right) \cdot \left(\frac{r}{\zeta}\right)^l \cdot \exp\left[-\frac{r^2}{2\zeta^2}\right]. \tag{14}$$

It should be noted that, for the mode $l \neq 0$, there exists a double degeneracy due to the two possible choices for the circular functions, [cos $(l\theta)$, sin $(l\theta)$]. Furthermore, for all modes, there exists an additional double degeneracy due to the scalar approximation. Therefore, the number of the propagating modes is twice the number of modes obtained from the scalar approximation.

The value of the parameter b which satisfies the stationary property is obtained from the condition;

$$d\beta_{lm}^2(b)/db = 0. \tag{15}$$

Substituting the solution b_0 of (15) into (11), we get

$$\beta_{lm}^2(b_0) = \hat{\beta}_{lm}^2(b_0) + k^2 n_0^2 \int_0^\infty f(r;b_0)\psi_{lm}^2(r;b_0) r\, dr \tag{16}$$

which satisfies the stationarity condition. In the following discussion, the letter b_0 will be omitted for simplicity since we treat only the solutions which satisfy the stationarity condition, so that $\beta_{lm}^2(b_0)$ and $f(r;b_0)$, for example, will simply be expressed hereafter as β_{lm}^2 and $f(r)$, respectively. The propagation constant of the (l,m) mode given by (16) must also satisfy the following condition:

$$\beta_{lm}^2 > (kn_2)^2. \tag{17}$$

III. Modal Dispersion

The delay time τ_{lm} of the pulse of the (l,m) mode after propagation along the fiber of length L is given by

$$\tau_{lm} = \frac{L}{c} \cdot \frac{dkn_0}{dk} \cdot \frac{d\beta_{lm}}{dkn_0} \tag{18}$$

where c is the velocity of light in free space. Neglecting material dispersion, (18) can be written as

$$\tau_{lm} = \frac{L}{c} \cdot n_0 \frac{d\beta_{lm}}{dkn_0}. \tag{19}$$

Because the delay times τ_{lm} for each mode are different, the input pulsewidth is broadened after propagation along the multimode fiber. To estimate the output pulsewidth for practical applications, let us introduce the standard deviation S of the normalized group delay of all propagating modes, defined by

$$S = \left(\frac{1}{M}\sum_{lm}\left[\frac{d\beta_{lm}}{dkn_0} - \left(\frac{1}{M}\sum_{l'm'}\frac{d\beta_{l'm'}}{dkn_0}\right)\right]^2\right)^{1/2} \tag{20}$$

where M is the total number of propagating modes, and $\sum$ denotes the sum over all propagating modes. The standard deviation S is related directly to the output pulse shape. The width $\Delta\tau$ over which the magnitude of the output pulse shape decays by a factor of $1/e$ is given approximately by

$$\Delta\tau = 3\frac{L}{c} \cdot n_0 S. \tag{21}$$

As we can see from the foregoing equation, the output pulsewidth is proportional to the standard deviation S. More precisely, the output pulsewidth is much more broadened than the input pulsewidth if the values of τ_{lm} disperse widely, whereas the input pulse retains almost its initial shape during its propagation along the fiber if the values of τ_{lm} are concentrated in a narrow range. In defining the standard deviation S given by (20) it is assumed that all propagating modes are uniformly excited at the sending end of the fiber. In the case of a nonuniform excitation, the

standard deviation of each group delay must be multiplied by an adequate weighting function. $d\beta_{lm}/dkn_0$ in (20) can be obtained from (11) as

$$\frac{d\beta_{lm}}{dkn_0} = \frac{1}{2\beta_{lm}} \cdot \frac{d\beta_{lm}^2}{dkn_0} = \frac{(1 - \frac{1}{2}A_{lm} + \frac{1}{2}(2B_{lm} + C_{lm}))}{(1 - A_{lm} + B_{lm})^{1/2}} \tag{22}$$

where

$$A_{lm} = 2(2m + l + 1)\sqrt{b_0}/kn_0$$

$$B_{lm} = \int_0^\infty f(r)\psi_{lm}^2(r) r\, dr$$

$$C_{lm} = kn_0 \frac{d}{dkn_0} \int_0^\infty f(r)\psi_{lm}^2(r) r\, dr. \tag{23}$$

The standard deviation S can easily be calculated by using (22).

IV. Numerical Examples and Discussions

Let us introduce the normalized frequency

$$\omega_n = kR\sqrt{\bar{n}_1^2 - n_2^2} \tag{24}$$

to treat the mode dispersion characteristics of various truncated parabolic-index fibers, where $\bar{n}_1$ is an equivalent refractive index of the core defined as

$$\bar{n}_1^2 = n_2^2 + \frac{2}{R^2} \int_0^R [n^2(r) - n_2^2] r\, dr. \tag{25}$$

The integral in the above equation must be carried out over the region of the core $n^2(r) > n_2^2$.

The normalized frequency ω_n is closely related to the number of the propagating modes. The propagation constants of the modes which have identical value of $(2m + l)$ are almost the same. Therefore, from (16) and (24), the normalized cutoff frequency of the mode group of order $N = (2m + l)$ is given approximately by

$$\omega_n = \sqrt{2}\,(N + 1). \tag{26}$$

Furthermore, the total number M of the propagating modes in a fiber which supports modes up to the Nth mode group is

$$M = (N + 1)(N + 2). \tag{27}$$

Figs. 2 and 3 show numerical examples of the frequency characteristics of $d\beta_{lm}/dkn_0$ for several lower $(0,m)$ modes, where the values of n_R/n_2 are (1.0, 0.997, 0.995) and (1.0, 1.003, 1.005), respectively, and $\bar{n}_1/n_2$ is equal to 1.01. As we can see from both figures, the values of $d\beta_{lm}/dkn_0$ depart from unity rapidly near the cutoff frequencies. Therefore, it is predicted that the mode dispersion characteristics would be affected (i.e., the pulsewidth is broadened) significantly by the propagating modes near cutoff. As shown in Fig. 2, in the case of $n_R/n_2 < 1$, the values of $d\beta_{lm}/dkn_0$ approach unity monotonically with increasing ω_n. In the case of $n_R/n_2 > 1$, on the other hand, the convergence of $d\beta_{lm}/dkn_0$ to unity is much slower as the value of n_R/n_2 increases as shown in Fig. 3.

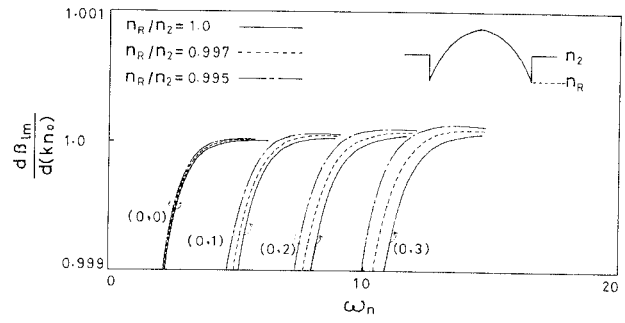

Fig. 2. Group delay $d\beta_{lm}/dkn_0$ versus normalized frequency ω_n with $n_R/n_2 \leq 1$ as a parameter.

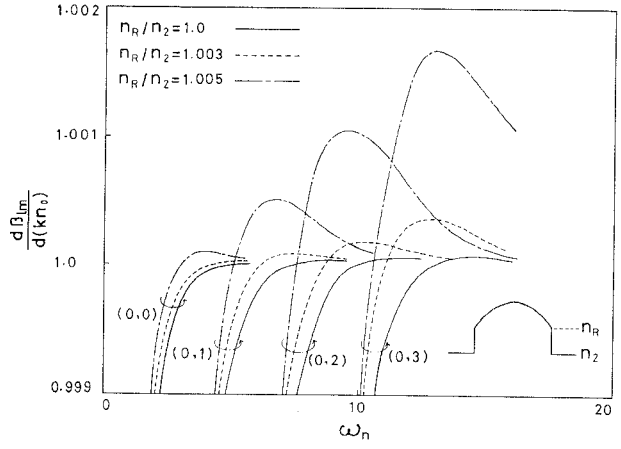

Fig. 3. Group delay $d\beta_{lm}/dkn_0$ versus normalized frequency ω_n with $n_R/n_2 \geq 1$ as a parameter.

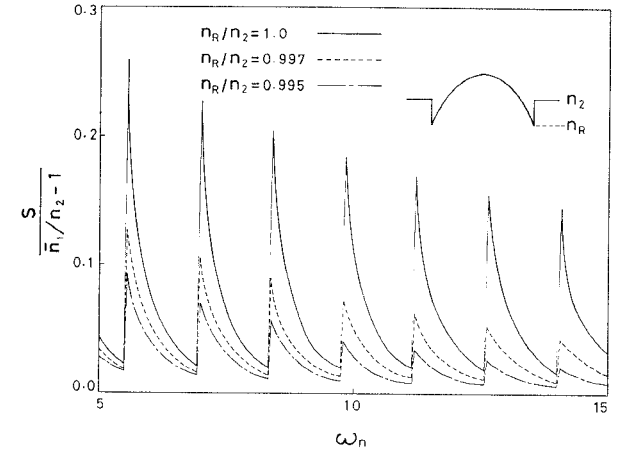

Fig. 4. Normalized modal dispersion $S/(\bar{n}_1/n_2 - 1)$ versus normalized frequency ω_n with $n_R/n_2 \leq 1$ as a parameter.

The frequency characteristic of the normalized standard deviation $S/[(\bar{n}_1/n_2) - 1]$ given by (20) are shown in Figs. 4 and 5, where the values of n_R/n_2 are assumed to be (1.0, 0.997, 0.995) and (1.0, 1.003, 1.005), respectively. In both figures, it is found that the standard deviation S varies abruptly and almost periodically. This feature is caused by the fact that new modes begin to propagate with increasing ω_n. This means that the output pulsewidth is significantly affected by the mode group near cutoff.

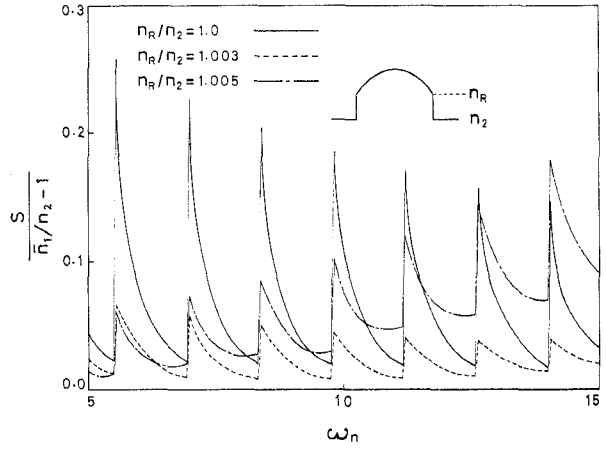

Fig. 5. Normalized modal dispersion $S/(\bar{n}_1/n_2 - 1)$ versus normalized frequency ω_n with $n_R/n_2 \geq 1$ as a parameter.

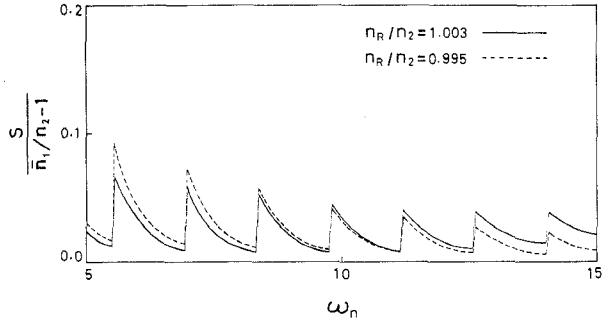

Fig. 6. Normalized modal dispersion $S/(\bar{n}_1/n_2 - 1)$ versus normalized frequency ω_n for the values of $n_R/n_2 = 1.003$ and $n_R/n_2 = 0.995$.

When the new mode group of order $(N + 1)$ begins to propagate, the number of the propagating modes increases by $2(N + 1)$. This is about $2/N$ times the total number of the propagating modes. Therefore, the influence on pulse broadening of the mode group near cutoff may be expected to decrease in general with the increase of N or ω_n. This is illustrated for a typical case with $n_R/n_2 < 1$ in Fig. 4, that is to say, the peak values of $S/[(\bar{n}_1/n_2) - 1]$ at the cutoff decrease monotonically for increasing ω_n when $n_R/n_2 < 1$.

However, when $n_R/n_2 > 1$, these peak values do not always decrease continuously for increasing ω_n but have a minimum at a value of ω_n which depends on the value of n_R/n_2, as we can see from Fig. 5. This is due to the fact that, in the case of $n_R/n_2 > 1$, the values of $d\beta_{lm}/dkn_0$ do not approach to unity monotonically and rapidly as mentioned previously in connection with Fig. 3. Furthermore it is found from Fig. 5 that S assumes a minimum for a particular value of ω_n. By contrast, in the case $n_R/n_2 < 1$, S does not assume a minimum value.

Two typical examples of the frequency dependence of the standard deviation S are shown in Fig. 6 where the values of n_R/n_2 are assumed to be 0.995 and 1.003. The standard deviation S for the fiber with $n_R/n_2 < 1$ is smaller than that for the fiber with $n_R/n_2 > 1$ at higher frequencies [3], whereas in the lower frequency region ($\omega_n < 10$ in our example), the situation is reversed. This means that a fiber

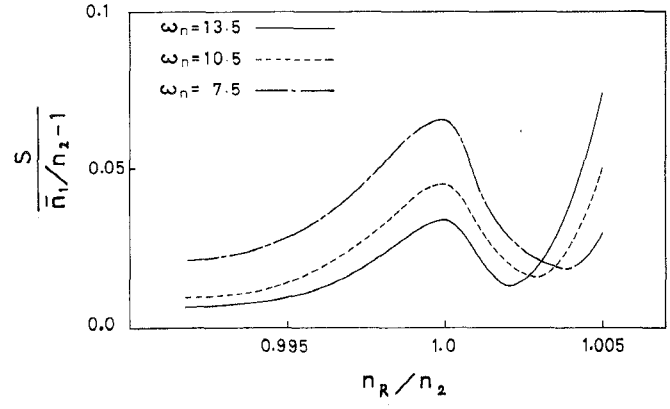

Fig. 7. Normalized modal dispersion $S/(\bar{n}_1/n_2 - 1)$ versus n_R/n_2 with normalized frequency ω_n as a parameter.

with an appropriate value of n_R/n_2 which is larger than unity can achieve better mode dispersion characteristics than a fiber whose value of n_R/n_2 is less than unity.

The relation between the standard deviation S and n_R/n_2 is shown in Fig. 7 with the normalized frequency ω_n as a parameter. The figure shows that, in the region $n_R/n_2 > 1$, S takes a minimum value for a particular value of n_R/n_2, whereas, in the region of $n_R/n_2 < 1$, S decreases monotonically as n_R/n_2 decreases. However, for n_R/n_2 values less than 0.995, S is almost constant and hence the mode dispersion characteristics are almost the same. Furthermore, as we can see from Fig. 7, the modal dispersion of fibers with $n_R/n_2 > 1$ for which S assumes a minimum is almost the same as that of fibers with $n_R/n_2 \simeq 0.995$.

Since the rate of change of the refractive index in the core becomes larger for smaller values of n_R/n_2, the energies of the propagating modes of a fiber with $n_R/n_2 < 1$ are trapped more tightly than in fibers with $n_R/n_2 > 1$. This makes it more difficult to connect fibers to each other. Therefore, from the practical point of view, fibers with n_R/n_2 greater than unity seem to be more desirable than fibers with $n_R/n_2 \simeq 0.995$ provided that the value of $n_R/n_2 (> 1)$ is chosen to minimize the modal dispersion. In addition, for improving the mode dispersion characteristics it is important that the fiber be operated at a frequency far from the cutoff of any mode groups.

V. Conclusion

The mode dispersion characteristics of the truncated parabolic-index fiber have been analyzed theoretically in detail by using a variational method. The standard deviation of the normalized group delay of the propagating modes has been used to estimate the modal dispersion behavior of the fiber. As a result, it has been shown that there exists an optimum index distribution of the truncated parabolic-index fiber at which the modal dispersion is minimized, and a minimum output pulsewidth broadening can be achieved.

In this paper, it has been assumed that fibers are free from losses. In a practical situation, however, the higher order modes near cutoff may be expected to suffer much more attenuation due to cladding and bending losses. Therefore, provided that the losses are taken into account, the influence

of these modes on the pulse broadening would be reduced to some extent.

References

[1] T. Uchida, M. Furukawa, I. Kitano, K. Koizumi, and H. Matsumura, "A light-focusing fiber guide," *IEEE J. Quantum Electron.*, vol. QE-5, p. 331, June 1969.

[2] D. Gloge, E. L. Chinnock, and K. Koizumi, "Study of pulse distortion in selfoc fibers," *Electron. Lett.*, vol. 8, pp. 526–527, Oct. 1072.

[3] Y. Suematsu and K. Furuya, "Refractive index distribution and group delay characteristics in multimode dielectric optical waveguides," *Trans. IECE Japan*, vol. 57-C, pp. 289–296, Sept. 1974.

[4] M. Matsuhara, "Analysis of TEM modes in dielectric waveguides by a variational method," *J. Opt. Soc. Amer.*, vol. 63, pp. 1514–1517, Dec. 1973.

[5] M. Geshiro, M. Ootaka, M. Matsuhara, and N. Kumagai, "Analysis of wave modes in slab waveguide with truncated parabolic index," *IEEE J. Quantum Electron.* (Corresp.), vol. QE-10, pp. 647–649, Sept. 1974.

[6] J. A. Stratton, *Electromagnetic Theory*. New York: McGraw-Hill, 1941, p. 343.

[7] P. M. Morse and H. Feshbach, *Methods of Theoretical Physics*. New York: McGraw-Hill, 1953, p. 1106.

Analysis of the Microstrip and the Electrooptic Light Modulator

MASANORI KOBAYASHI

Abstract—**Green's function for examples with anisotropic media is obtained using the image-coefficient method. The method is based on the boundary conditions and the reciprocity relation. Using this Green's function and solving directly the charge distribution on the strip, the line capacitances per unit length of a microstrip and of an electrooptic light modulator are obtained. High accuracy of this method is demonstrated by comparing the present results with the results obtained using the conformal mapping and with other data appeared in the literature. The charge distributions are also illustrated. Of particular interest is the effective filling fraction of the dielectric material, which depends mainly on the shape ratio and only slightly on the relative dielectric constant. The effective filling fractions are tabulated for the microstrip with a homogeneous dielectric substrate.**

List of Symbols

ε_0	Permittivity of free space (vacuum).
$\bar{\varepsilon}$	Permittivity tensor of anisotropic material.
ε_x^*, ε_y^*	Relative dielectric constants of anisotropic material in the directions of x-axis and y-axis, respectively.
ε^*	Relative dielectric constant of isotropic material.
$\varepsilon_{\text{eff}}^* = \dfrac{C/\varepsilon_0}{C_0/\varepsilon_0}$	Effective relative dielectric constant.
$q_w = \dfrac{\varepsilon_{\text{eff}}^* - 1}{\varepsilon^* - 1}$	Wheeler's effective filling fraction.
C	Capacitance per unit length of microstrip or of electrooptic light modulator.
C_0	Capacitance per unit length of line without dielectric.
q	Line charge.
σ	Charge distribution on the conductor.
m	Number dividing the conductor.
γ	Constant of 1, 2, or 3.
N	Truncated number of the infinite series in Green's function.
K	$= \dfrac{\sqrt{\varepsilon_{2x}^*\varepsilon_{2y}^*} - \sqrt{\varepsilon_{1x}^*\varepsilon_{1y}^*}}{\sqrt{\varepsilon_{2x}^*\varepsilon_{2y}^*} + \sqrt{\varepsilon_{1x}^*\varepsilon_{1y}^*}}$ image coefficient.
$\psi(q, \varepsilon_x^*, \varepsilon_y^*, \theta)$	Electric flux per unit angle emitted from the source line charge q in the radial direction with the angle θ from the x-axis.
α	$= \alpha_2/\alpha_1 (\alpha_1 = \sqrt{\varepsilon^*{}_{1y}/\varepsilon^*{}_{1x}}\ \alpha_2 = \sqrt{\varepsilon^*{}_{2y}/\varepsilon^*{}_{2x}}$.
$Z_c = \sqrt{\mu_0/\varepsilon_0}$	Intrinsic impedance of the free space (vacuum).

Manuscript received March 1, 1977; revised June 27, 1977.

The author is with the Department of Electrical Engineering, Faculty of Engineering, Ibaraki University, Hitachi, Ibaraki, 316 Japan.

I. Introduction

THE CALCULATION of the parameters of a microstrip line based on a TEM approximation is useful for the design of microwave integrated circuit structures [1]–[8]. The parameters can be derived from the line capacitance. The method in [1] is based on modified conformal mapping. The methods in [2], [3], [5]–[8] use Green's function satisfying the boundary conditions. The method in [4] is based on the relaxation technique. Isotropic substrate

0018-9480/78/0200-0119$00.75